Proceedings of the 2009 IEEE
International Conference on Robotics and Biomimetics
December 19 -23, 2009, Guilin, China

Mathematical Modeling of Brain Circuitry during Cerebellar Movement Control

Henrik Jörntell, Per-Ola Forsberg, Fredrik Bengtsson & Rolf Johansson, *Member, IEEE*

Abstract— **Reconstruction of movement control properties of the brain could result in many potential advantages for application in robotics. However, a hampering factor so far has been the lack of knowledge of the structure and function of brain circuitry *in vivo* during movement control. Much more detailed information has recently become available for the area of the cerebellum that controls arm-hand movements. In addition to previously obtained extensive background knowledge of the overall connectivity of the controlling neuronal network, recent studies have provided detailed characterizations of local microcircuitry connectivity and physiology *in vivo*. In the present study, we study one component of this neuronal network, the cuneate nucleus, and characterize its mathematical properties using system identification theory. The cuneate nucleus is involved in the processing of the sensory feedback evoked by movements. As a substrate for our work, we use a characterization of incoming and outgoing signals of individual neurons during sensory activation as well as a recently obtained microcircuitry characterization for this structure. We find that system identification is a useful way to find suitable mathematical models that capture the properties and transformation capabilities of the neuronal microcircuitry that constitute the cuneate nucleus. Future work will show whether specific aspects of the mathematical properties can be ascribed to a specific microcircuitry and/or neuronal property.**

I. Introduction

In order to understand and describe how the brain organizes limb movement control, we aim to design a mathematical model of this control. The study is based on a comprehensive neurophysiological characterization of the cerebellar system for voluntary arm-hand control as described by Apps and Garwicz [1]. This system may be viewed as a vast network of interconnected neurons that involves many parts of the brain, which all are interconnected through a specific area of the cerebellum [13, 2]. A foundation for the model system is a previous, detailed characterization of all constituent neuron types and a systematic description of connectivity patterns both within the cerebellum and in those brain regions outside the cerebellum, which are part of the network devoted to this specific control as shown is previous publications from our group [3, 14, 4, 15, 17, 2].

H. Jörntell, Per-Ola Forsberg and Fredrik Bengtsson are with Lund University, Section for Neurophysiology, Dept. Experimental Medical Science, BMC F10 Tornavägen 10, SE-221 84 Lund, Sweden (e-mail Henrik.Jorntell@med.lu.se)

R. Johansson is with Lund University, Dept. Automatic Control, PO Box 118, SE-22100 Lund Sweden, (e-mail Rolf.Johansson@control.lth.se)

As for detailed electrophysiological neuron modeling, the Goldman-Hodgkin-Katz voltage equation (or the Goldman equation) is the standard model used in cell membrane physiology to determine the equilibrium potential across a cell membrane, taking into account all the relevant ion species active through that membrane [18].

Brain function may be viewed as a result of the transformation functions of individual neurons and their precise interconnections. However, the network of neurons that constitute the brain is very well organized into discrete subcomponents. Each subcomponent is connected to a limited set of other subcomponents in specific, well-conserved connectivity patterns. Viewed in this way, it is possible to make a control system-inspired interpretation of the function of the brain in movement control [7, 19, 21, 22, 23, 24] and we can interpret the neuronal system for arm-hand movement control as being organized into a number of distinct functional units, in a similar fashion as a control system. Each functional unit, or subcomponent of brain circuitry, hence has a specific function, which can be expressed in mathematical terms. In the case of the brain, this function is carried out by a limited set of neuron types, which typically can have relatively simple internal circuitry connectivity.

Conversely, a mathematical problem formulation of optimal control problem and related adaptive control with tentative solutions were published in [9].

In the present study, we aim to provide a mathematical description of the function of one of these functional subunits, namely the cuneate nucleus, which carries out the first order processing of movement-generated sensory feedback. We illustrate the firing patterns of the primary afferents, main cuneate neurons and the local inhibitory interneurons and how system identification methods can be used to obtain a mathematical expression of the function carried out by the cuneate nucleus. In ongoing work, we also simulate in detail how the underlying neuronal information processing is carried out, with the aim of providing neuroscientific correlates for specific features in these mathematical expressions.

II. Problem formulation

Since our approach rests on the understanding of the biological system, i.e. the brain, much work needed to be devoted the collection of the biological data. The data

978-1-4244-4775-6/09/$25.00 © 2009 IEEE.

collection should be from primary afferents, *i.e.*, nerve fibers which mediate sensory input from peripheral receptors to the central nervous system, from the main neurons of the cuneate, which project the processed sensory information to the cerebellum [2]. Ideally, we should record from the primary afferent and its target cuneate neuron simultaneously, but this is technically very difficult. An approximation is to record from primary afferents and cuneate neurons driven by the same inputs. To compare the primary afferent data with the data from the cuneate neurons, comparisons should only be made between primary afferents and neurons which are activated by the same modality of sensory information and from sensory input activated from the same topological area (on the skin or in the joints/muscles). If we can fulfill these criteria, we can take advantage of previous findings suggesting that single primary afferents can have a dominant influence on the cuneate neuron [5]. The transformation taking place between the primary afferent input and the cuneate neuron output for a given stimulus can then be characterized through system identification.

In order to verify that the mathematical model obtained accurately represents the transformation between the primary afferent and the cuneate neuron in the more general case, data from both primary afferent and cuneate neuron should also be obtained from a very different type of stimulus. If the mathematical model is correct, it should be able to reproduce the input-output transformation also in this case.

III. Materials & Methods

The experiments were carried out with single unit metal microelectrodes and patch clamp recordings in the acute animal preparation of the decerebrated cat as described in [15, 2]. Primary afferent axons were recorded on their pathway into the cuneate nucleus and cuneate neurons were recorded inside the cuneate nucleus. Stimuli were delivered in two different ways. The first, which was used to produce the model through the system identification, was a standardized manual skin stimulation. A miniature strain gauge device was mounted on the tip of the investigator in order to control that the same amount of force and the same stimulation time was used. A second mode of stimulus was electrical skin stimulation applied through a pair of needle electrodes inserted into the skin with a spacing of 3 mm. Stimulation intensity was 1.0 mA, duration 0.1 ms.

As for empirical model estimation, standard methods and validation methods of system identification were used [10].

Then, the recorded data were processed using an action potential pattern recognition software, in order to reduce noise. For every action potential, only the time after stimulation was determined, transforming data to spike-time data. This in turn could be added over several stimulations, yielding histogram data. This was then exported to Matlab. For the mathematical modeling of the neuron transmission, the Matlab System Identification Toolbox was used [20]. Various different model structures were tested—*e.g.,* PEM, ARX, ARMAX, OE, BJ, N4SID [20]—to determine the model which provided the most accurate representation. The starting point was to find the model which most accurately represented the transformation for a standardized manual skin stimulation. Subsequently, we simulated the primary afferent input evoked by electrical skin stimulation and compared the simulated cuneate neuron response with actual responses recorded from the cuneate neuron with the same electrical skin stimulation.

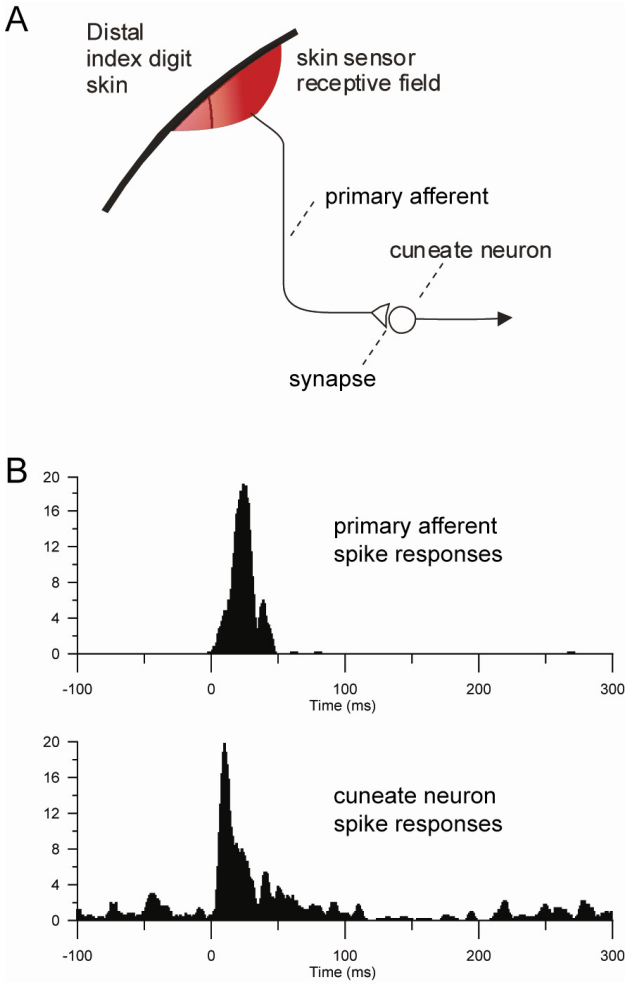

Figure 1: (A) Cartoon illustrating the central parts of the experimental setup. Cuneate neurons receive input from primary afferents, which in turn are excited from peripheral receptors (in this case the skin of the distal index finger or digit) and make excitatory synapses on the cuneate neuron. (B) Using the same, standardized manual skin stimulation, data for the spike responses evoked in primary afferents and cuneate neurons were stored as peristimulus histograms (bin width 1 ms, stimulation started at time 0). The duration of the stimuli in this case was indicated to be 50 ms by the strain gauge device.

IV. Results

Figure 1 illustrates the spike responses of a primary afferent and a cuneate neuron to manual skin stimulation. The data is displayed as peristimulus histograms, i.e. the same stimulation was repeated many times and the spike counts for each bin represent the sum of spike responses for 30-50 consecutive, near identical, stimuli. All stimuli were aligned so that they start at 0 ms and ended at 50 ms. The primary afferent, which conveys the input to the cuneate neuron via a synapse (Fig. 1A), display spikes only on stimulation. Therefore the time before the stimulation is devoid of spikes, even though the spike response to the stimulation is quite intense (Fig. 1B, top). In contrast, the cuneate neuron has a spontaneous activity, hence the spike activity before the stimulation, and in addition seem to have a more intense spike response to stimulation (note steep increase in spike activity immediately after the onset of the stimulation, Fig. 1B, bottom).

In the next step, we simulated that the primary afferent input was driven by electrical skin stimulation. This type of stimulation evokes a precisely timed primary afferent spike, about 4.5 ms after the stimulation, with a near 100% fidelity and a coefficient of variation of 0% (at 0.1 ms resolution) (data not shown). Figure 2 illustrates the actual cuneate neuron response when this primary afferent spike input was evoked experimentally.

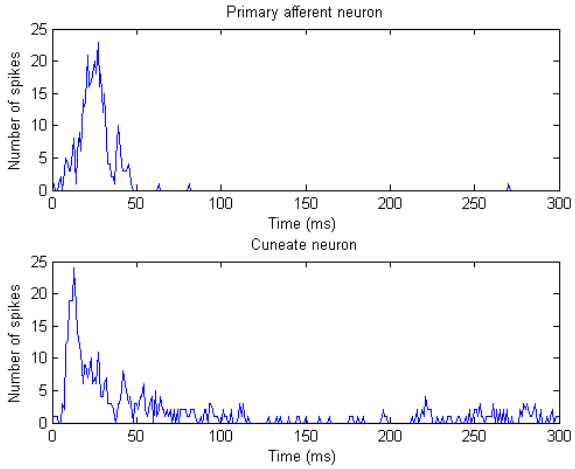

Figure 2: Primary afferent spike responses (*upper diagram*) and cuneate neuron spike responses to electrical skin stimulation.

Figure 2 illustrates the actual cuneate neuron response when this input was evoked experimentally (*upper diagram*) and the experimental response (*lower diagram*) evoked by a single pulse input comparable to the spike response of the real primary afferents (Fig. 3B).

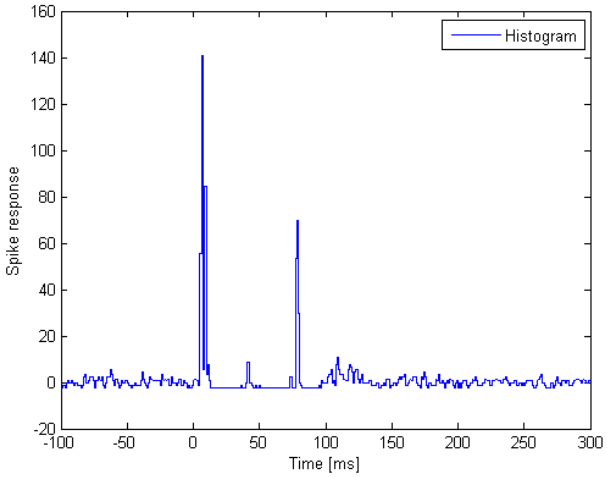

Figure 3: Spike response recorded from a cuneate neuron subject to electrical skin stimulation.

Figure 3 exhibits the spike response recorded from a cuneate neuron subject to electrical skin stimulation.

The traces illustrated in Fig. 4 show the simulated response of the mathematical model with the best fit. Interestingly, this model quite well captured the fast variations in the initial part of the response but failed to capture the subsequent inhibitory response that followed the initial excitation. It also failed to capture the release from the inhibitory response (at 200 ms+). These two late phases of the response are likely generated by the local inhibitory interneurons of the cuneate nucleus.

With the necessary data at hand, we next attempted to use system identification to find an appropriate mathematical model representing the transformation of the information conveyed by the primary afferent to the cuneate neuron. We found that a prediction error estimate, discrete-time state space model (PEM) of fifth order gave the best fit, on the form of a state-space model:

$$\begin{aligned} x_{k+1} &= Ax_k + Bu_k + Kw_k \\ y_k &= Cx_k + w_k \end{aligned}$$

The fit for the PEM, ARX, ARMAX, OE, BJ and N4SID models were 66%, 61%, 66% 64% and 64%, respectively. The estimated state-space model

$$\begin{aligned} x_{k+1} &= Ax_k + Bu_k + Kw_k \\ y_k &= Cx_k + w_k \end{aligned}$$

with the system matrices

$$A = \begin{bmatrix} 1.0281 & 0.1103 & -0.0329 & -0.0179 & -0.0476 \\ 0.0078 & 0.9167 & 0.1257 & -0.0376 & 0.5252 \\ -0.0744 & -0.0056 & 0.8474 & 0.3213 & -0.0070 \\ -0.0002 & -0.0528 & -0.4983 & 0.7843 & 0.0813 \\ -0.0207 & -0.1959 & -0.0113 & -0.3575 & 0.7903 \end{bmatrix}$$

$$B = \begin{bmatrix} 0.0027 \\ -0.0163 \\ -0.0004 \\ -0.0095 \\ 0.0018 \end{bmatrix},\ K = \begin{bmatrix} 0.0026 \\ 0.0022 \\ 0.0033 \\ 0.0070 \\ -0.0039 \end{bmatrix}$$

$$C = [20.5466 \quad -9.6495 \quad 4.4225 \quad 1.8089 \quad 5.8488]$$

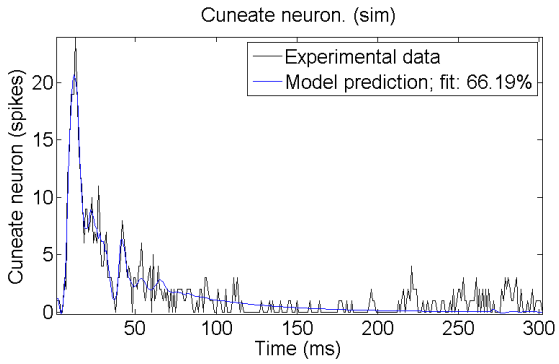

Figure 4: Recorded (black trace) and simulated response (blue trace) of a cuneate neuron to primary afferent response shown in Fig. 1B.

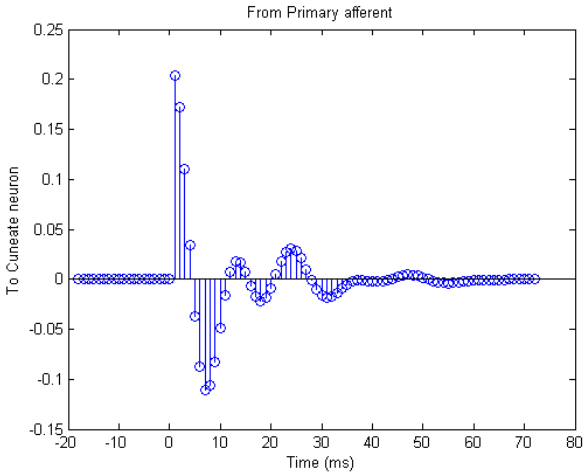

Figure 5: Impulse response for the prediction-error model model (PEM) in the form of a state-space model of the cuneate spike response.

Figure 5 shows the impulse response for the prediction-error model model (PEM) in the form of a state-space model of the cuneate spike response. In this case, the fit between the experimental data and the prediction accuracy of the simulation appears to be very high, although the temporal relationships seem to need some further refinements of the model. In the recorded data (Fig. 3) the spontaneous firing activity of the cuneate neuron provides a background against which also inhibitory effects in the neuron can be recorded (as a temporary depression of the spontaneous firing activity). This occurs immediately after the initial excitatory response. In the model, inhibition is represented by negative output, something which is not possible in the brain for neurons that make excitatory synapses (which is the case for the cuneate neurons which make excitatory synapses with neurons of the cerebellum and thalamus). However, spontaneous background activity also participates in determining the spike output of the downstream neurons (*i.e.*, in the cerebellum and thalamus) so the reduction of this background activity can actually be viewed as being equivalent to negative output. Therefore, we can conclude that the mathematical model well reflects the response properties of the primary afferent-to-cuneate neuron junction. Since it is able to do so for two widely different inputs (manual skin stimulation that evokes a primary afferent spike response lasting 50 ms and electrical skin stimulation which evokes a spike response lasting for 0.1 ms) it promises to be able to account for the response properties over a wide range of inputs and perhaps covering the majority of the physiological range of inputs.

As an illustration of model variability, Fig. 6 shows the impulse response corresponding to electrical skin stimulation for the ARX model. It is evident that these models do not capture the cuneate neuron firing mechanics in response to electrical stimulation as the PEM model did. These empirical mathematical models are on the form

ARX:

$$A(z)y_k = B(z)u_k + w_k$$

OE:

$$y_k = \frac{B(z)}{F(z)}u_k + w_k$$

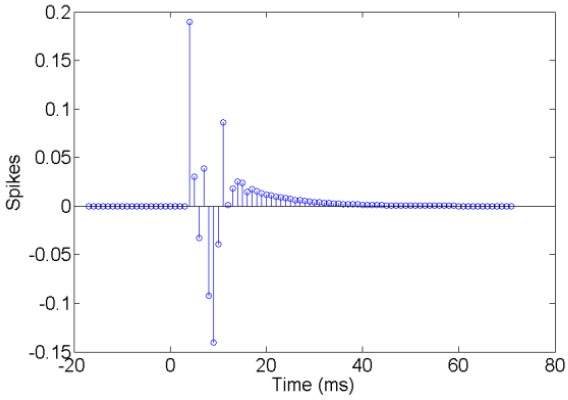

Figure 6: Impulse response for the ARX model.

Figure 7 shows the Bode diagram of the PEM model. Interestingly, the diagram shows deriving properties for a large part of the spectrum with phase lead. These are favourable properties from a control systems point of view. This indicates that these properties could be important features of the cuneate neuron, in its role of transforming sensory information from primary afferent neurons to the cerebellum, which in turn can be viewed as a controller of body movements.

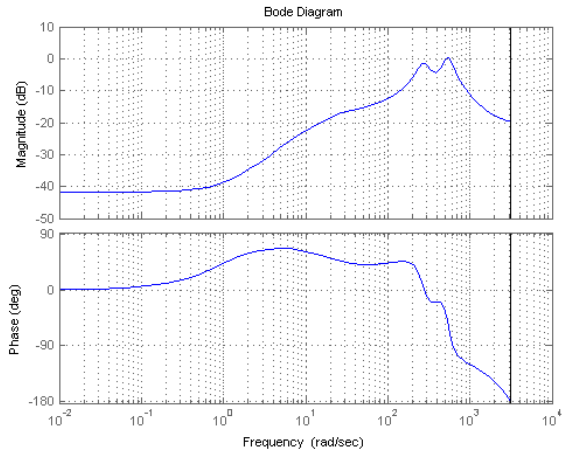

Figure 7: Bode diagram of the PEM model model of the cuneate spike response. It is interesting to note that the model exhibits differentiating properties and phase lead for a part of the spectrum, indicating that these properties could be important features of the cuneate neuron.

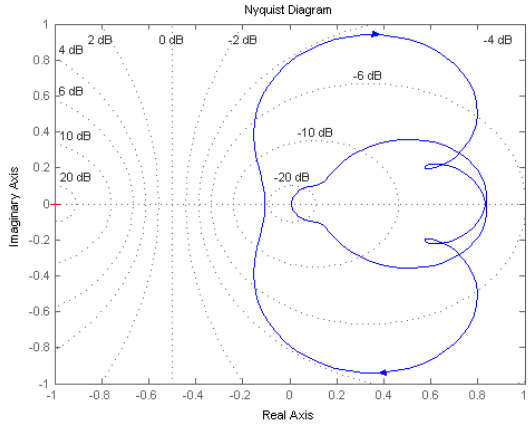

Figure 8: Nyquist diagram of the PEM model model of the cuneate spike response including closed-loop gain level surfaces for the cuneate spike response. It is interesting to note that the model shows differentiating properties and phase lead for a part of the spectrum, indicating that these properties could be important features of the cuneate neuron.

Finally, Ho-Kalman impulse response model reproducing cuneate histogram spike-response data was made with high modeling accuracy (Fig. 9). Note that also the long-term response was reproduced by the model.

V. Discussion

Based on the findings of Figs. 5, 7-8, the empirical cuneate model exhibits differentiating characteristics, suggesting a phase-lead action of the cuneate response. When a longer impulse response is considered (Fig. 8), the differentiating aspects are less pronounced.

V. Conclusions

Our preliminary findings suggest that system identification can be used to identify the mathematical properties of a local neural structure with an uncomplicated network structure. The failure to reproduce the later phases of the response to manual skin stimulation (Fig. 2) can be explained by the fact that this response occurred well after the cessation of the primary afferent spike train. In the brain, this type of response is likely created by the local inhibitory interneurons, which is an input that was not 'known' to the model. Future modelling experiments will show whether the addition of this factor can make the model reproduce also this aspect of the response.

Based on these findings and the previous experimental results of Jörntell and Bengtsson [2-4, 13-17], further modeling of neural structures—inside and outside the cerebellum in order to understand control system aspects—could potentially give new insights into cerebellar movement control. This aspect—*i.e.*, how the cerebellum achieves movement control—could be of great interest not only in the field of neuroscience, but in robotics and other control applications as well.

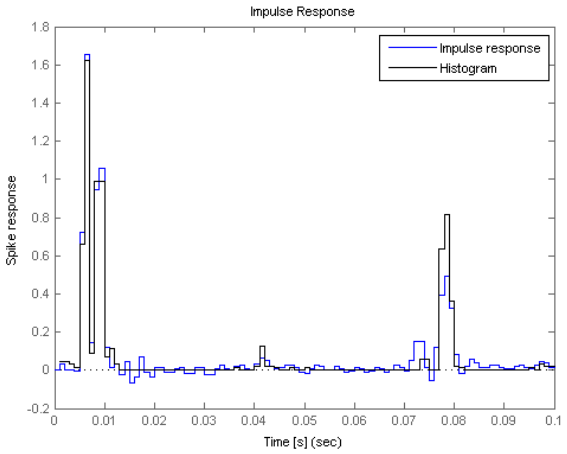

Figure 9: Ho-Kalman impulse response model (*blue graph*) reproducing cuneate histogram spike-response data (*black graph*).

References

[1] Apps R, Garwicz M (2005) Anatomical and physiological foundations of cerebellar information processing. *Nature Reviews: Neuroscience* 6:297-311.

[2] Bengtsson F, Jorntell H (2009) Sensory transmission in cerebellar granule cells relies on similarly coded mossy fiber inputs. *Proc Natl Acad Sci USA* 106:2389-2394.

[3] Ekerot CF, Jorntell H (2001) Parallel fibre receptive fields of Purkinje cells and interneurons are climbing fibre-specific. *Eur J Neurosci* 13:1303-1310.

[4] Ekerot CF, Jorntell H (2003) Parallel fiber receptive fields: a key to understanding cerebellar operation and learning. *Cerebellum* 2:101-109.

[5] Ferrington DG, Rowe MJ, Tarvin RP (1987) Actions of single sensory fibres on cat dorsal column nuclei neurones: vibratory signalling in a one-to-one linkage. *J Physiol* 386:293-309.

[6] Fujita M (1982) Adaptive filter model of the cerebellum. *Biological Cybernetics* 45:195-206.
[7] Ito M (1972) Neural design of the cerebellar motor control system. *Brain Res* 40:81-84.
[8] Ito M (2008) Control of mental activities by internal models in the cerebellum. *Nat Rev Neurosci* 9:304-313.
[9] R. Johansson. Quadratic optimization of motion coordination and control. *IEEE Transactions on Automatic Control*, 35(11):1197--1208, 1990
[10] R. Johansson. *System Modeling and Identification***.** Prentice Hall, Englewood Cliffs, NJ, 1993.
[11] R. Johansson and M. Magnusson. Optimal coordination and control of posture and locomotion. *Mathematical Biosciences*, 103:203--244, 1991.
[12] R. Johansson. Adaptive control of robot manipulator motion. *IEEE Transactions on Robotics and Automation*, 6(4):483--490, 1990.
[13] Jorntell H, Ekerot CF (1999) Topographical organization of projections to cat motor cortex from nucleus interpositus anterior and forelimb skin. *Journal of Physiology* (London) 514 (Pt 2):551-566.
[14] Jorntell H, Ekerot CF (2002) Reciprocal bidirectional plasticity of parallel fiber receptive fields in cerebellar Purkinje cells and their afferent interneurons. *Neuron* 34:797-806.
[15] Jorntell H, Ekerot CF (2003) Receptive field plasticity profoundly alters the cutaneous parallel fiber synaptic input to cerebellar interneurons in vivo. *Journal of Neuroscience* 23:9620-9631.
[16] Jorntell H, Ekerot CF (2006) Properties of somatosensory synaptic integration in cerebellar granule cells in vivo. *Journal of Neuroscience* 26:11786-11797.
[17] Jorntell H, Hansel C (2006) Synaptic memories upside down: bidirectional plasticity at cerebellar parallel fiber-Purkinje cell synapses. *Neuron* 52:227-238.
[18] Junge, D (1981). *Nerve and Muscle Excitation* (2nd edition ed.). Sunderland, MA: Sinauer Associates. pp. 33–37
[19] Kawato M, Gomi H (1992) A computational model of four regions of the cerebellum based on feedback-error learning. *Biological Cybernetics* 68:95-103.
[20] L. Ljung, System Identification Toolbox for Matlab, MathWorks, Natick, MA, 2002.
[21] Miall RC, Wolpert DM (1996) Forward models for physiological motor control. *Neural Networks* 9:1265-1279.
[22] Schweighofer N, Arbib MA, Kawato M (1998a) Role of the cerebellum in reaching movements in humans. I. Distributed inverse dynamics control. *European Journal of Neuroscience* 10:86-94.
[23] Schweighofer N, Spoelstra J, Arbib MA, Kawato M (1998b) Role of the cerebellum in reaching movements in humans. II. A neural model of the intermediate cerebellum. *Eur J Neurosci* 10:95-105.
[24] Wolpert DM, Miall RC, Kawato M (1998) Internal models in the cerebellum. *Trends in Cognitive Science* 2:338-347.